

Structural and Functional Imaging of Engineered Tissue Development using an Integrated OCT and Multi-Photon Microscope

Lester J. Fahrner^a, Wei Tan^a, Claudio Vinegoni^a, Thomas E. Eurell^b, Stephen A. Boppart^{a, c, d}

^aBeckman Institute for Advanced Science and Technology, Urbana, IL, 61801

^bDepartment of Veterinary Biosciences, U. of Illinois, Urbana, IL, 61801

^cDepartment of Electrical and Computer Engineering, U. of Illinois, Urbana, IL, 61801

^dCollege of Medicine, U. of Illinois, Urbana, IL, 61801

ABSTRACT

Recent advances in the field of tissue engineering have led to the development of complex three-dimensional tissue constructs. It has become clear, however, that the traditional tools used for studying standard cell cultures are not always adequate for diagnostically studying thick, highly-scattering cultured tissues. Furthermore, many techniques used for studying three-dimensional constructs are invasive or require exogenous fluorophores, which damage the tissue and prevent time-course studies of tissue development. An integrated optical coherence tomography (OCT) and multi-photon microscope (MPM) has been constructed for visualizing 3-D engineered tissues. OCT was used for imaging structure and cell organization, while MPM was used for assessing functional properties of cells. We demonstrate technical developments involved in the construction of this instrument and its use in the non-destructive investigation of cell movement and tissue organization in engineered tissues. Cells labeled with GFP and exogenous fluorescent probes have also been imaged with OCT and confocal microscopy. Studies indicate that an integrated microscope has the potential to be an enabling diagnostic tool for future studies in the growth and organization of engineering tissues and in cell-cell and cell-matrix interactions.

Keywords: Tissue Engineering, Optical Coherence Tomography, Multiphoton Microscopy

1. INTRODUCTION

The field of tissue engineering has had many successes over the last decade [1-3]. Despite these successes, there are still many challenges ahead. One necessary challenge lies in the shift from 2-D to 3-D cell cultures for tissue engineering, as 3-D cultures demonstrate a more biologically-relevant range of function and activity [4]. Another challenge involves maximizing our understanding of the structural and functional organization of the tissue we are trying to create. While various imaging techniques such as histology, SEM, and TEM have been employed to ascertain these tissue properties, their destructive nature makes them inadequate for time-course studies of tissue development. Non-invasive technologies that are capable of deep imaging into 3-D cultures allow for a more comprehensive picture of various tissues.

Optical Coherence Tomography (OCT) is one example of recent technology that has been used extensively for understanding tissue properties and imaging tissues [5-7]. Similarly, Multiphoton Microscopy (MPM) has been used high-resolution cellular imaging [8-13]. Given the proven abilities of these techniques individually, and their complementary nature, we find it natural to combine the two into a single instrument, and apply the instrument to the study of engineered tissues so we can develop a more accurate understanding of the processes and structures involved in the growth, development, and responses of engineered tissues. Current research demonstrates the successful use of integrated imaging systems for biological studies [14,15].

OCT and MPM can potentially employ the same source of light. A femtosecond pulsed laser provides this light, which most commonly is a mode-locked titanium:sapphire laser operating at a center wavelength of around 800 nm. Near-infrared light penetrates deep into tissue, compared to light in the visible spectrum, as these wavelengths fall into the

“biological window” of tissue. OCT relies on the low-coherence source to attain a high imaging resolution, while MPM requires a high peak laser intensity (achieved with ultrashort pulses) to produce nonlinear multiphoton effects. The high-resolution, non-invasive imaging deep into tissue provided by OCT and MPM enables the study of tissue growth and repair.

OCT provides information on the structure of an object by detecting light that is reflected back to the objective by scattering. In tissue, OCT has the potential to image at the level of cells, nuclei, extracellular matrix, and blood vessels. MPM, much like confocal or fluorescence microscopy, images biological specimens by detecting re-emitted (fluorescent) light from an absorbing material. In confocal or fluorescence microscopy, short-wavelength light (488 nm, for example) excites certain molecules to an excited state. The excited molecules subsequently relax to a lower vibrational energy level, then emit light as they transition to a ground state. The emitted light is of a longer wavelength (lower energy) than the excitation light because of the energy lost in the vibrational energy level change. In a multiphoton microscope, high-intensity light with a longer wavelength (800 nm, for example) is sent through an objective into tissue. A photon at this longer wavelength is incapable of exciting the desired molecules to a higher energy level. Occasionally, however, two photons rather than one are absorbed within a short period of time. These two photons have the same effect as one shorter-wavelength photon, and the molecule is excited to a higher energy level. As in confocal microscopy, the molecule relaxes to a lower vibrational energy level, and then emits light as it transitions back to the ground state. Certain molecules, such as exogenous fluorescent probes, are capable of excitation from high-intensity light of a specific wavelength, and are commonly used in cell and tissue growth studies [16]. These markers can be attached to a specific protein in a cell, and if the protein is active, then the marker is expressed as well, and fluorescence can be detected. A variety of naturally-occurring molecules in tissues are also fluorescent, and can autofluoresce (e.g. NADPH), creating a background fluorescence that is occasionally observed [9].

A microscope incorporating both methods allows image correlation. By overlaying the structural image from OCT on the functional (i.e. an exposed fluorescent marker implies a functional protein) image from MPM, a more comprehensive view of a tissue can be obtained. In these studies, we explore the use of OCT and MPM for observing focal adhesions between cells in a chitosan scaffold [17,18], follow the injury and structural remodeling of damaged engineered tissues, and demonstrate the use of an integrated OCT and multiphoton microscope in cell growth studies.

2. MATERIALS AND METHODS

2.1 Observation of cell growth using GFP-labeled vinculin

Mouse NIH-3T3 cells from the American Type Culture Collection (ATCC) were transfected with a custom-made GFP-labeled vinculin (courtesy of Dr. Geiger of the Weizmann Institute, Israel). Previous studies with this labeled protein have allowed the study of mechanical forces inherent in cell interaction, growth, and replication [19]. In this preliminary analysis, we determine whether the transfected cells proliferate, and whether we can detect the expressed GFP with confocal microscopy. Specifically, cells were grown on a chitosan scaffold over the course of 7 days in a microincubator (LU-CPC, Harvard Apparatus), and were observed one, three, and seven days after culture with OCT and a laser scanning confocal microscope (DM-SP2, Leica Microsystems). An OCT image of the chitosan scaffold can be seen in Figure 1. The average pore size was approximately 100 μm , which was an appropriate size for cells to attach to the three-dimensional scaffold and proliferate into the pores.



Figure 1: OCT images of chitosan structure. Scale bar is 200 μm

The laser source of the OCT system is an 80MHz repetition-rate pulsed titanium:sapphire (Ti:Al₂O₃) laser (Lexel 480, Lexel Laser) that is pumped by a Nd:YVO₄ ($\lambda=532$ nm) solid-state laser (Coherent Verdi V-5). The Ti:Sapphire laser provides 450 mW of power with a center wavelength of 800 nm over a full-width half-max (FWHM) bandwidth of 15 nm (corresponding to a coherence time of 130 fs) in a Gaussian-shaped pulse and spectrum. This pulsed beam is directed into an ultrahigh-numerical aperture (UHNA) optical fiber (UHNA3, Thorlabs, Inc.), where nonlinear effects of the fiber spread the FWHM bandwidth to greater than 100 nm (corresponding to a depth (axial) resolution of 3 microns) [20]. The beam is subsequently split with a 50/50 fiber-based optical coupler (Gould Fiber Optics). One path exiting the coupler is directed to the sample, where a 12 mW beam from the fiber is collimated, steered with linear scanning galvanometers (Cambridge Technology, Cambridge, MA), and focused with an aspheric lens to a 10 μm diameter spot (transverse resolution). The other path exiting the coupler is directed to a reference arm, where the beam from the fiber is collimated, passed through dispersion-compensating glass, and is sent to a retroreflector that is mounted on a scanning delay galvanometer that moves 2mm repetitively at 25Hz. Light from each path of the system is reflected (or scattered and reflected) and returns to the splitter. The light is recombined, and the resulting interference signal is detected by a fiber-based photodetector (Model 2007 New Focus, Inc.). A data acquisition board (PCI-6110, National Instruments) captures and digitizes this signal with 12-bit accuracy for display and processing on a computer. This OCT system can image up to 2mm into a weakly-scattering substance such as the chitosan scaffold. OCT was used to determine the structure of the chitosan scaffold and the structure of the 3T3 cells overlying the scaffold. Imaging multiple times over 7 days allowed the study of subsequent changes of these structures.

Confocal fluorescence microscopy was performed using an inverted microscope (DM-IRE2, Leica Microsystems) with a Laser Scanning Confocal Microscope (LSCM) attachment (TCS-SP2, Leica Microsystems). The system acquired images with a 63x objective (0.70 NA) at up to 3 frames per second. Data from photomultiplier tubes (PMTs) was digitized with 12-bit precision for display on a computer. Multiple PMTs and fluorophores allowed the overlay of pseudo-colored images to produce one composite multicolored image. An argon laser with $\lambda=488$ nm excited the GFP. Fluorescence of naturally occurring cellular components or exogenous probes is possible with other laser lines provided by the same LSCM.

2.2 Damage and remodeling of engineered tissues

Engineered corneal equivalents previously developed for the study of laser and chemical damage using traditional imaging and histological methods were used in this study [21]. These equivalents are produced from rabbit keratocytes and epithelial cells (Cascade Biologics in Portland, OR). A transwell (Costar) cell culture insert with a polycarbonate membrane is seeded with a stromal fibroblast and liquid-collagen solution and placed in a multi-well plate to gel into a type of extracellular matrix. A layer of stratified squamous epithelial cells is grown over the extracellular matrix. The combination of these two tissue types, as in Figure 2, creates a valuable model for investigating the properties of natural cornea.

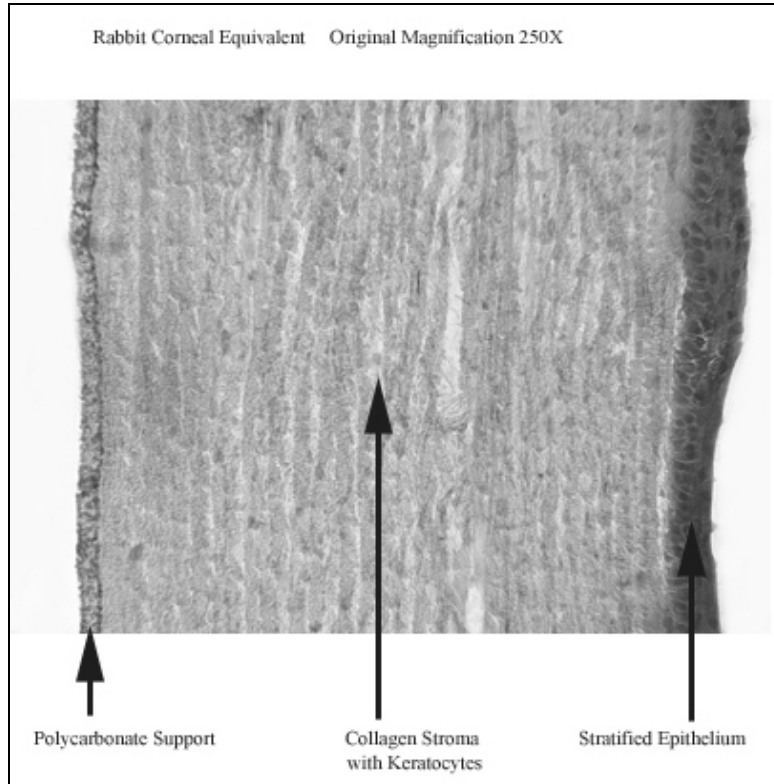


Figure 2: Histology of engineered corneal equivalent

For this study, 4 groups of 3 equivalents each were used: 3 groups of 3 equivalents each were exposed to different damaging stimuli, while the fourth group of 3 equivalents was used as a control group. The exact exposures can be seen in Table 1 below. For this preliminary study, the equivalents in Group 3 (base-damaged) were exposed to different concentrations due to a larger-than-expected amount of damage that was caused by the first 5N exposure. The B and C equivalents in Group 3 were exposed to a less concentrated KOH solution to more closely match the physical extent of damage caused in Group 2 (acid-damaged group).

Table 1: Exposure levels for corneal equivalents.

	Group 1	Group 2	Group 3	Group 4
	Control	Acid	Base	Laser
A	CONTROL	1 μ L 1N Acetic Acid for 1.5 min	2 μ L 5N KOH for 3 min	1.5 W 532nm CW for 1.5 min
B	CONTROL	1 μ L 1N Acetic Acid for 1.5 min	1 μ L 1N KOH for 2 min	1.5 W 532nm CW for 1.5 min
C	CONTROL	1 μ L 1N Acetic Acid for 1.5 min	1 μ L 1N KOH for 1 min	1.5 W 532nm CW for 1.5 min

A solid-state continuous-wave laser (Coherent Verdi V-5) with a wavelength of 532 nm was used to damage the tissue. A 1.5 W beam was directed through a 10x/0.25NA objective to achieve a theoretical spot size of 11 μ m in diameter. The observed damage zone, however, was on the order of 0.5 mm in diameter. The discrepancy may be due to the amount of time that the equivalent was exposed to the laser, which may have caused the surrounding area to be damaged as well. Multiple similar laser exposures were made on each of the Group 4 (laser-damaged) equivalents to

ensure that sufficient damage had occurred. Different spots were imaged each day to obtain an overall perspective of changes in the tissue.

The damaged and control equivalents were imaged within 12 hours after initial exposure. Parameters for the OCT imaging system are the same as those in the previous section. After imaging, all equivalents including the controls were submerged in Dulbecco's modified Eagle medium (DMEM) (BioWhittaker) and 5x antibiotic/antimycotic solution (segregated by group) to reduce the chance of contamination. The DMEM solution was discarded after 30 minutes, and more DMEM with 5x antibiotic/antimycotic was added as growth media. The samples were placed in a cell/tissue incubator until the next OCT imaging session. This process was repeated daily for 6 days. Afterwards, the imaged samples were frozen, sectioned, and underwent standard histological processing with hematoxylin and eosin staining for light microscopy visualization of the damage and repair processes.

2.3 Integrated microscope implementation

A custom-built free-space OCT and MPM microscope has been constructed from a modified upright light microscope (Axioplan II, Carl Zeiss, Inc.). Major changes to the original microscope include the addition of a computer-controlled three-dimensional stage (Mac 5000, Ludl Electronics Products) for sample scanning in an *en face* plane, and a camera port on top of the microscope for laser-delivery and detection of the reflected OCT and multi-photon fluorescent signals. A rigid aluminum frame was built around the microscope to stabilize the microscope and to provide mounting points for various optomechanical components.

The OCT and MPM functions of this microscope share a laser source (Lexel 480, Lexel Laser), sample beam delivery optics, motion control hardware, and data acquisition tools. Differences between the two functions lie in light collection methods: OCT uses a photodetector located at a position that allows sample light to interfere with a reference arm signal, while MPM uses optical filters and a photomultiplier tube (PMT) to detect photons at a different wavelength than the source beam.

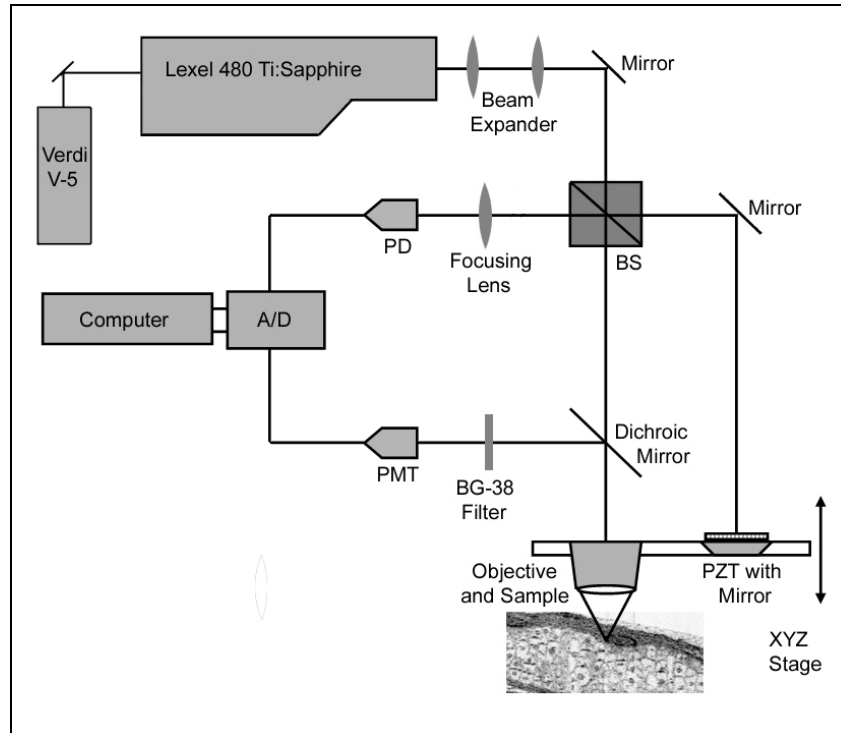


Figure 3: Schematic of combined OCT-MPM microscope

Figure 3 shows a schematic of this system. The titanium:sapphire pulsed laser (FWHM bandwidth=15 nm) is directed into a beam expander and a cube beamsplitter to separate the sample and reference paths of the OCT setup. The reference path incorporates a one-axis stage that creates a path length delay in order to achieve interference by matching this path with the sample arm path, and it terminates in a mirror that is mounted on a piezoelectric stack. This piezoelectric stack (Karl Stetson Associates, LLC) is controlled by a 5.6 kHz sinusoidal signal from a function generator and amplifier to modulate the reference arm distance by about $2*\lambda$ (1600nm). The reflected beam travels back along the same path to the beamsplitter. The sample arm path is directed into the top of the microscope, where it passes through a dichroic mirror. This dichroic mirror transmits light with wavelengths longer than 650 nm (-3dB point), and reflects at shorter wavelengths. Theoretically, then, the first pass through the dichroic mirror should not reduce the power of the beam. The beam continues to the objective, where it is focused to a spot. An objective mount allows multiple objectives to be used. In this experiment, a 50x, 0.5 NA long working-distance objective (442850, Carl-Zeiss, Inc.) was used, which produced a 0.9 micron diameter spot (OCT transverse resolution).

Photons that are scattered directly back by a scattering object or an interface in the sample return to and are collected by the objective. These photons pass through the dichroic mirror again since they are still at a wavelength of 800 nm, and travel back to the beamsplitter. Both beams (reference and sample) are directed out of the beamsplitter and focused onto a photodetector (DET-110, Thorlabs, Inc), where interference between the two beams occurs.

The MPM function of the microscope uses the sample beam through the same objective as OCT, but photons are absorbed by an excitable material rather than scattered and re-emitted as either single or two-photon fluorescence. Two-photon fluorescence returning to the objective is at a shorter wavelength than the 800 nm excitation light, and is therefore diverted by the dichroic mirror through a BG-38 color filter (CVI Laser, LLC) that minimizes stray 800 nm photons. The remaining (shorter-wavelength) photons are detected by a photomultiplier tube (PMT) (H7421-50, Hamamatsu).

A low-noise preamplifier (SR-650, Stanford Research Systems) filters and amplifies the OCT signal. Data acquisition on both analog OCT and MPM signals is performed using a PC-based device (Labjack U12, Labjack Corporation). Digitized signals are processed and presented with a custom control software package.

3. RESULTS AND CONCLUSIONS

3.1 Cell growth

Figure 4 shows a sample confocal microscope image from the GFP-vinculin study on cell growth and adhesion. Results of the study show that the formation of focal attachments between growing cells occurs in three-dimensional chitosan scaffolds, and that these changes can be detected with confocal microscopy. Figure 5 shows representative top-view (*en face*) OCT microscope images of the structure of a chitosan scaffold.

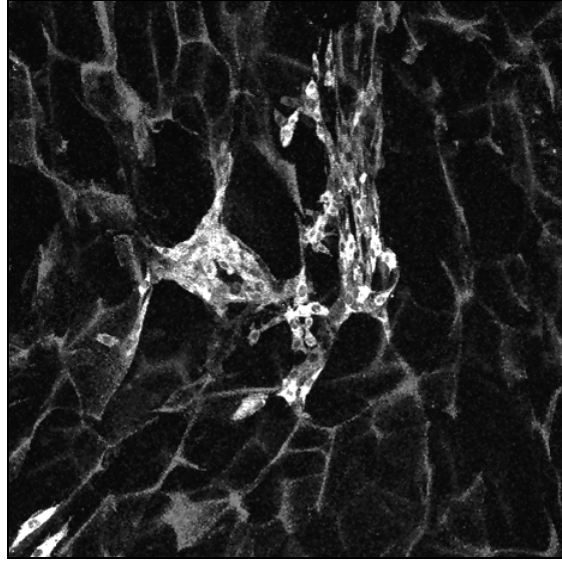


Figure 4: Confocal microscopy image of cell and tissue structure. Brighter areas correspond to GFP-tagged vinculin, while darker structure corresponds to the autofluorescing chitosan scaffold.

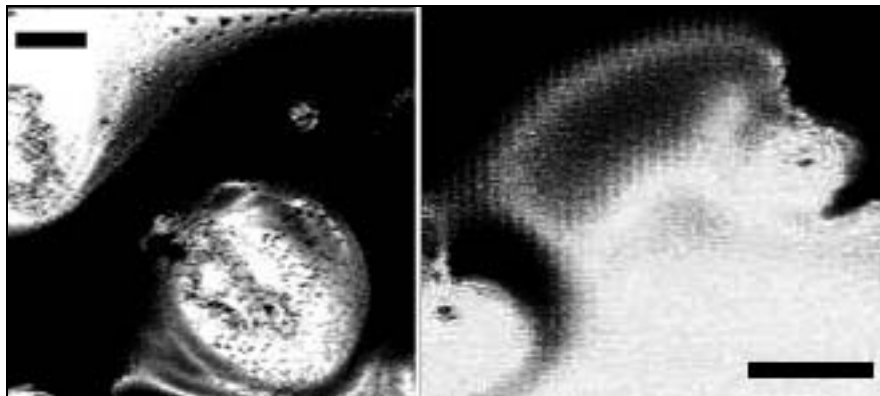


Figure 5: *En face* OCT microscope images of chitosan structure. Scale bars are 50 μm .

3.2 Tissue damage

Figure 6 is a compilation of images taken over a six-day period. The control samples appear to maintain the same structure throughout the period. The acid-damaged samples seem to have a damaged area that is more-scattering but also more uniform than healthy tissue. The epithelial layer seems to have a constant thickness, and the connective tissue seems to have a constant height as well, but the cells within the epithelial layer were possibly destroyed during the initial exposure. The base-damaged samples responded differently to exposure than the acid-damaged samples. The liquefactive effect of the KOH seems to have dissolved or somehow changed the connective tissue below the epithelium, although the top surface of the sample remains relatively even. The laser-damaged samples show a highly-scattering (possibly thermally-damaged) region that shadows the underlying connective tissue region, creating the impression of a cone-shaped hole. Over the course of the study, it appears that the damaged area changes such that the scattering is reduced, which results in a smaller and less-prominent shadow.

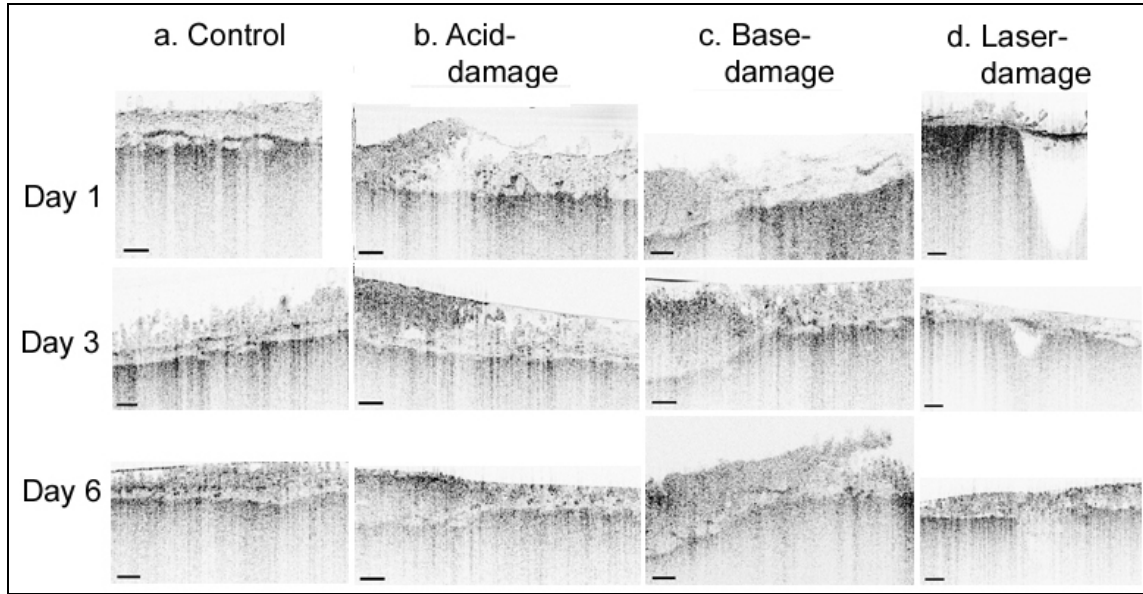


Figure 6: OCT of change in engineered cornea over time with different damage methods. Scale bars = 100 μm . The damage in (b) and (c) is located on the left side of the images, while the right side appears undamaged to the eye

3.3 Integrated OCT and MPM imaging

The integrated microscope obtained OCT images with a theoretical transverse resolution of less than one micron, with a calculated confocal parameter of 1.6 μm , and with a coherence length of 19 μm . MPM images had a FWHM transverse resolution of 0.6 μm , while the FWHM depth resolution was 3.75 μm . To demonstrate edge-definition of this microscope, sample images of a machined metal template are provided in Figure 7. The square holes (on a raised area) in the metal device are 76 μm on a side.

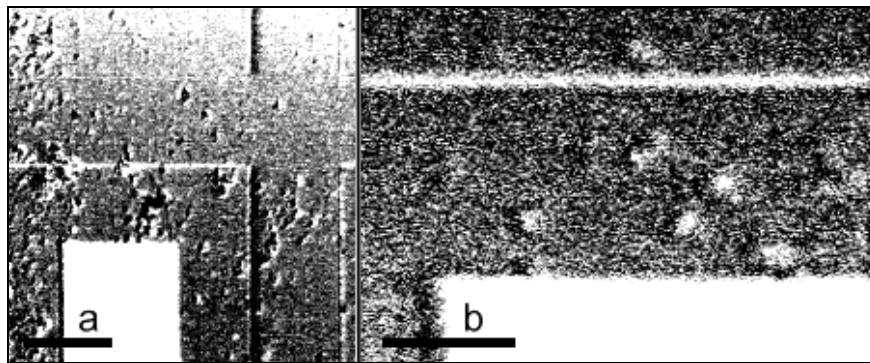


Figure 7: *En face* OCT of metal device (a) Scale bar = 50 μm (b) Scale bar = 20 μm

Figure 8 shows images of corresponding structure and fluorescence in a celery test specimen. The fluorescent dye was not transfected in this case; rather, a drop was placed topically on the sample, and after 1 minute of diffusion through the tissue, the sample was imaged with the integrated OCT/MPM microscope. The OCT image of the sample in Figure 8a shows that the cell walls of the structure scatter incident light and therefore produce obvious features in the

image. Figure 8b shows the corresponding MPM image in which fluorescent dye is shown to be present in the extracellular space. The area shown in these images may be collenchyma or sclerenchyma, a tissue type notable for unevenly-thick cell walls that provides mechanical strength to the celery. This possibility is considered because of the areas of very high scattering and absorption of the dye between cells.

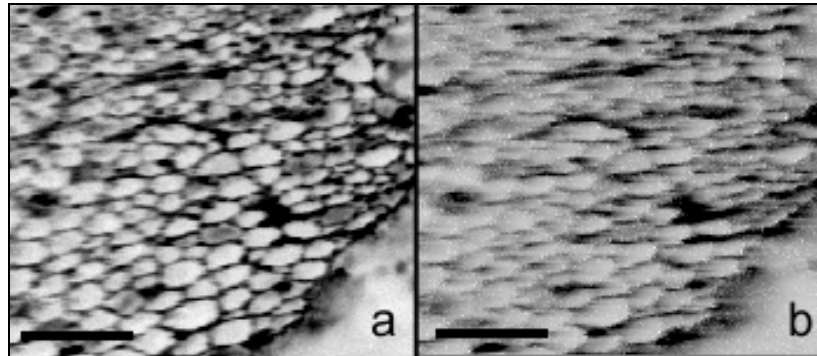


Figure 8: Corresponding celery (a) *en face* OCT and (b) MPM images. Scale bar = 50 μm

The images in Figure 9 demonstrate the use of the integrated microscope for correlating structural and functional information from cell cultures. Despite the large number of confluent cells that are visible in Figure 9a, only a few cells contain the Hoechst dye. The faint diagonal line (arrows) in Figure 9b may demarcate an area with autofluorescence of the unlabeled cells or perhaps a residual amount of dye from lysed cells. Images of corresponding structure and fluorescent markers in engineered tissue are promising tools in the improvement of our understanding of tissue interaction, development, remodeling, and function.

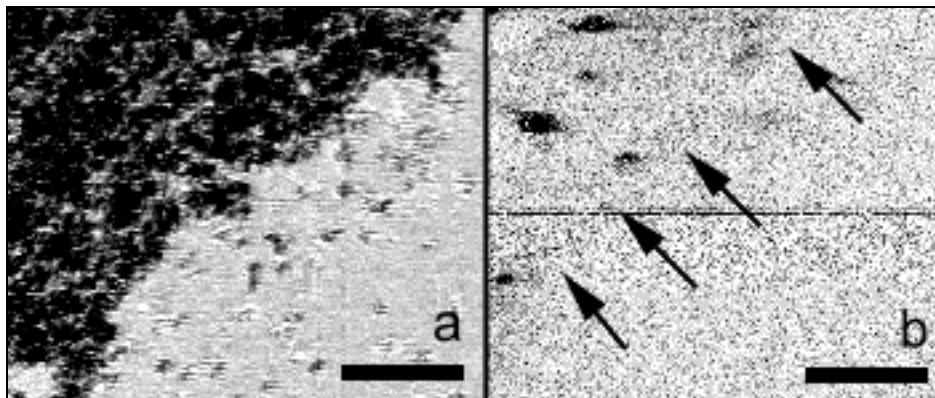


Figure 9: Corresponding 3T3 fibroblast (a) *en face* OCT and (b) MPM images. Hoechst dye was added as an exogenous fluorophore. Arrows indicate edge of confluent cells. Scale bar = 50 μm

ACKNOWLEDGMENTS

This work was supported in part by the National Institutes of Health (1 R01 EB00108-1), the National Science Foundation (BES-0086696), the UIUC Critical Research Initiative, and the Beckman Institute.

REFERENCES

1. R. Langer and J.P. Vacanti, "Tissue Engineering", *Science*, pp. 920-926. 1993.
2. L.E. Niklason and R. Langer, "Advances in tissue engineering of blood vessels and other tissues," *Transplant Immun*, pp. 303-6. 1997.
3. M. Griffith, R. Osborne, R. Munger, X. Xiong, C.J. Doillon, N.L.C. Laycock, M. Hakim, Y. Song, M.A. Watsky, "Functional human corneal equivalents constructed from cell lines," *Science*, pp. 2169-72. 1999.
4. E. Cukierman, R. Pankov, D.R. Stevens, K.M. Yamada, "Taking cell-matrix adhesions to the third dimension," *Science*, pp. 1708-12. 2001.
5. D. Huang, E.A. Swanson, C.P. Lin, J.S. Schuman, W.G. Stinson, W. Chang, M.R. Hee, T. Flotte, K. Gregory, C.A. Puliafito, J.G. Fujimoto, "Optical Coherence Tomography," *Science*, pp. 1178-1181. 1991.
6. S.A. Boppart, B.E. Bouma, C. Pitris, J.F. Southern, M.E. Brezinski, and J.G. Fujimoto, "*In vivo* cellular optical coherence tomography imaging," *Nature Medicine*, pp. 861-5. 1998.
7. J. Fujimoto, "Optical coherence tomography for ultrahigh resolution *in vivo* imaging", *Nature Biotech*, pp. 1361-1367. 2003.
8. W. Denk, J.H. Strickler, W.W. Webb, "Two-photon laser scanning fluorescence microscopy," *Science*, pp. 73-6. 1990.
9. W.R. Zipfel, R.M. Williams, W.W. Webb, "Nonlinear magic: multiphoton microscopy in the biosciences", *Nature Biotech*, pp. 1369-1377, 2003.
10. C. Xu, W. Zipfel, J.B. Shear, R.M. Williams, W.W. Webb, "Multiphoton fluorescence excitation: New spectral windows for biological nonlinear microscopy," *Proc. Natl. Acad. Sci. USA*, pp. 10763-68. 1996.
11. K. Konig, "Multiphoton microscopy in life sciences", *J Microscopy*, pp. 83-104. 2000.
12. B.R. Masters, P.T.C. So, E. Gratton, "Multiphoton excitation microscopy of *in vivo* human skin," *Ann NY Acad Sci*, pp. 58-67. 1998.
13. P.T.C. So, C.Y. Dong, B.R. Masters, K.M. Berland, "Two-photon excitation fluorescence microscopy," *Ann Rev Biomed Eng*, pp. 399-429. 2000.
14. E. Beaurepaire, L. Moreaux, F. Amblard, J. Mertz, "Combined scanning optical coherence and two-photon-excited fluorescence microscopy", *Opt Letters*, pp. 969-971, 1999.
15. J.P. Dunkers, M.T. Cicerone, N.R. Washburn, "Collinear optical coherence and confocal fluorescence microscopies for tissue engineering," *Optics Express*, pp. 3074-3079. 2003.
16. R.Y. Tsien, "The green fluorescent protein", *Ann Rev Biochem*, pp. 509-544. 1998.
17. B.M. Gumbiner, "Cell adhesion: The molecular basis of tissue architecture and morphogenesis," *Cell*, pp. 345-57. 1996.
18. W. Tan, R. Krishnaraj, T.A. Desai, "Evaluation of nanostructured composite collagen-chitosan matrices for tissue engineering," *Tissue Engineering*, pp. 203-10. 2001.
19. N.Q. Balaban, U.S. Schwarz, D. Riveline, P. Goichberg, G. Tzur, I. Sabanay, D. Mahalu, S. Safran, A. Bershadsky, L. Addadi, B. Geiger, "Force and focal adhesion assembly: a close relationship studied using elastic micropatterned substrates," *Nat Cell Biol*, pp. 466-472. 2001.
20. D.L. Marks, A.L. Oldenburg, J.J. Reynolds, S.A. Boppart, "Study of an ultrahigh-numerical-aperture fiber continuum generation source for optical coherence tomography," *Optics Letters*, pp. 2010-2. 2002.
21. T.E. Eurell, J.M. Sinn, P.A. Gerding, C.L. Alden, "*In vitro* evaluation of ocular irritants using corneal protein profiles," *Toxicol Appl Pharmacol*, pp. 374-8. 1991.